ISSN 1750-9823 (print)
International Journal of Sports Science and Engineering
Vol. 01 (2007) No. 03, pp. 165-176

Modeling the Influence of Crew Movement on Boat Velocity Fluctuations during the Rowing Stroke

Nicholas Caplan [1, +] and Trevor Gardner [2]

[1] School of Psychology and Sport Sciences, Northumbria University, Newcastle upon Tyne, UK.
[2] School of Sport and Exercise Sciences, University of Birmingham, Birmingham, UK.

(*Received August 20 2007, accepted September 2 2007*)

Abstract. Caplan and Gardner (2007: Journal of Sports Sciences, 25, 1025-1034) presented a rowing simulation which assumed that each rower moved as a single mass. Although validated against mean on-water shell velocity, instantaneous velocity was not modeled well. As any changes to rowing technique inherently influence the fluctuations in boat velocity throughout each stroke, the previous model was unable to fully explore the influences of technique on the progression of the boat during each stroke. The present study aimed to address this limitation by implementing a five-segment model of each crew member, in order to better simulate the movement of each body segment throughout each stroke, and the influence this movement has on boat velocity fluctuations. A Vicon motion analysis system was used to collect kinematic data of nine sub-elite club rowers rowing on a Concept 2 model C rowing ergometer, from which mean joint trajectories were extracted for the ankle, knee, hip, shoulder, elbow and hand. From this data, kinematic relationships were determined to model the motion of the rowers for input into the simulation. The single segment and five-segment models were validated against previously published on-water mean boat velocity. Both models showed a close agreement with the measured on-water data, although the agreement was improved for the five-segment model. When compared to instantaneous velocity during one stroke for on-water rowing, the five-segment model was seen to better simulate the main features of the on-water data, which were not seen with the single segment model. This development of the model could have practical applications to rowers, coaches and sports scientists as individual rower kinematics could be used to estimate the influence of their technique (or technique changes) on both mean boat velocity and the velocity profile during each stroke.

Keywords: rowing, kinematics, model, motion analysis, momentum

1. Introduction

Many authors have reported on the factors influencing rowing performance, including the propulsive forces generated by the rowers (Caplan & Gardner, 2005; Spinks, 1996; Owen et al., 2002; Hartmann et al., 1993), rower kinematics (Barrett & Manning, 2004; Holt et al., 2003; McGregor et al., 2004), the influence of rowing ability (Smith & Spinks, 1995; Elliott et al., 1993), feedback systems designed to improve rower training (Hawkins, 2000; Smith & Spinks, 1998; Smith & Loschner, 2002), and equipment design (Caplan & Gardner, 2007a; Caplan & Gardner, 2007c; O'Brien, 1970; Scragg & Nelson, 1993; Pelham et al., 1993). However, the influence of crew movement patterns on the boat velocity fluctuations seen during each stroke are not so clearly understood. Martin and Bernfield (1980) first reported an increase in boat velocity during the recovery of the stroke which was attributed to the relative movement of the crew backwards in the boat when the oar blades were extracted from the water. Due to the momentum exchanges occurring between crew and boat throughout the stroke, this increase in sternwards motion of the rowers caused a concomitant increase in bow-wards velocity of the boat. During the drive phase crew movement would act to slow the boat down, although less noticeably due to the propulsive force generated at the oar blades.

Kleshnev (1999) presented measured on-water boat velocity data for a heavyweight men's eight. This data illustrates the fluctuations in boat velocity throughout a complete stroke (Fig. 1). It can be seen that the velocity initially decreases, until the propulsive forces generated by the rower are sufficient to overcome the drag forces and the forces exerted on the boat by the bow-wards motion of the crew. Towards the end of the drive phase the boat velocity plateaus. This can be explained through an examination of the movement

[+] *E-mail*: nick.caplan@unn.ac.uk

patterns of the different body segments. At this stage the legs are at full extension and will thus no longer contribute to propulsion. The forces generated by the rotating trunk and arm actions will also reduce as these segments approach the limits of their motion, and would decrease below the level of resistive forces generated by water and air and by crew momentum.

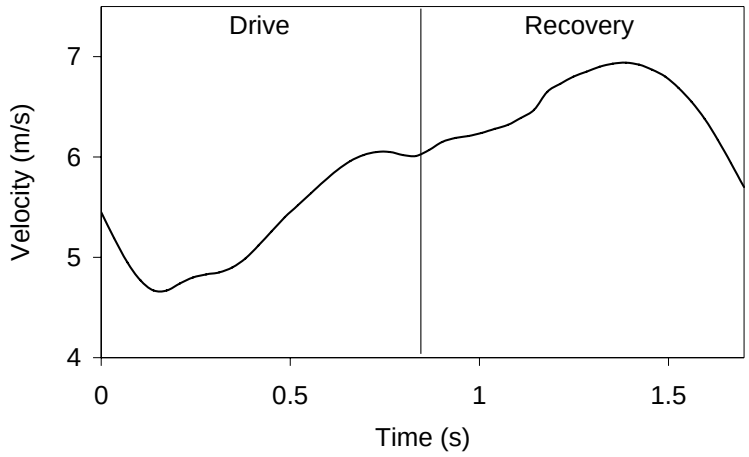

Fig. 1. Boat velocity profile for a complete stroke at 36 strokes per minute for a heavyweight men's eight (from Kleshnev, 1999). Drive and recovery phases are indicated and were determined by the change in direction of oar shaft rotation.

During the recovery phase, the oar blades are extracted from the water so only the relative crew motion can contribute to propulsion. After an initial slow rise in boat velocity, the velocity increases to a maximum just after half way through the phase and then slows towards the end of the stroke. The initial slow rise in boat velocity can be explained by the lack of movement of the legs into flexion at the start of the recovery. The legs must wait until the hands are passing the knees, otherwise the trajectory of the oar blade will be impaired. This results in only the relatively small mass of the arms moving sternwards at the start of the recovery (and to some extent the trunk), and hence the change in momentum will be small. The increased rate of acceleration seen one third of the way through the recovery would indicate the start of knee flexion. Towards the end of the recovery boat velocity slows as rower momentum reduces and resistive forces dominate.

Due to the natural variability of any biological system, it is often desirable to model such systems mathematically in order to isolate specific variables to perform controlled tests. A number of mathematical models of rowing have appeared in the literature which accommodate the movement of the crew within the boat in different ways (Millward, 1987; Brearley & de Mestre, 1996; Brearley et al., 1998; Caplan & Gardner, 2007b; Cabrera et al., 2006). Millward (1987) assumed that the rowers remained stationary relative to the boat. As this is not the case in the modern racing boat, the lack of crew movement resulted in a poor simulation of boat velocity as the boat simply slows throughout the recovery because no momentum exchange occurs between the stationary crew and boat.

Brearley and de Mestre (1996) and Brearley et al. (1998) realized the impact of this limitation and modelled the crew moving back and forth as a single mass with half of simple harmonic motion about their centre of mass location. Although modeled boat velocity fluctuations were improved, this model was also in that the oar blades were assumed to remain locked in the water during the drive phase despite the oar blades actually following a complex path through the water, acting as aerofoils (Affeld et al., 1993; Colloud et al., 2001; Nolte, 1993).

More recently, Caplan and Gardner presented a series of papers (Caplan & Gardner, 2007a; Caplan & Gardner, 2007b; Caplan & Gardner, 2007c) which determined the fluid dynamic properties of various oar blades and modeled the actual movement of the oar blade through the water to better predict rowing performance. However, whilst the model was valid against measured mean on-water boat velocity, crew movement was still modeled as a single mass moving with simple harmonic motion and so the model was limited in its prediction of instantaneous boat velocity throughout each stroke.

Cabrera (2006) further developed the modeling of crew movement. Kinematic relationships were provided which used the positions of the hip and shoulder in the direction of boat movement to determine the

centre of mass location, with this position being assumed to be a fixed proportion of the distance between the hip and shoulder position. Although both shoulder and hip positions were used to estimate the centre of mass position, the model still assumed a single mass moving back and forth, and did not determine the centre of mass location of each body segment of the lower and upper limbs and the trunk.

The aims of the present study, therefore, were to develop a five-segment kinematic model of crew movement which calculated the centre of mass positions of the shank, thigh, trunk, upper arm and forearm for each crew member, and which accounted for their individual contributions to boat velocity during each rowing stroke. It was hypothesized that the key features of the velocity profile of a boat throughout a complete stroke would be better simulated by the five-segment model when compared to the previously published single segment model (Caplan & Gardner, 2007b).

2. General model derivation

In rowing, propulsive force must be applied to the boat to overcome the various sources of resistance, and the crew should be able to move back and forth within the boat. Thus the equation of motion, following Newton's second law, can be written as:

$$P - D = m\frac{dv_{shell}}{dt} + M(\frac{dv_{crew}}{dt} + \frac{dv_{shell}}{dt}) \quad (1)$$

where m is the mass of the shell, oars and coxswain, M is the combined mass of the crew, vshell is the velocity of the shell, vcrew is the velocity of the crew relative to the boat, P is the propulsive force which is calculated by modeling the fluid dynamic interactions between the oar blades and water during the drive phase of stroke (Caplan & Gardner, 2007b) and D is the drag force, which is proportional to the velocity of the boat. The assessment of drag uses coefficients determined experimentally by Wellicome (1967) for the shell drag of an eight, and the relationship for air drag presented by Hoerner (1965) for a seated man multiplied by the number of rowers (Caplan & Gardner, 2007b). Equation (1) can now be rewritten to make boat acceleration the subject of the equation such that

$$\frac{dv_{shell}}{dt} = \left(P - D - M\frac{dv_{crew}}{dt} \right) \Big/ \left(m + M \right) \quad (2)$$

Although there will be lateral forces applied to the boat due to the rotational motion of the oar shaft and the forces applied to the oar handle, the model assumes that the same lateral forces will be applied by the rowers on both sides of the boat, such that they will cancel each other out. It is also acknowledged that the attitude of the boat will fluctuate through the stroke due to the forward and backwards oscillations of the crew and hence the combined centre of mass of the boat and crew. However, in order to model this accurately would require a detailed examination of the hydrodynamic drag of the boat which is beyond the scope of this investigation.

3. Modelling crew movement

Equation (2) illustrates that the force exerted on the boat by crew movement is given by the product of their mass and acceleration relative to the boat. Caplan and Gardner (2007b) previously assumed that all crew members moved in perfect synchrony, acting as a single mass moving back and forth with half of simple harmonic motion, as previously presented by Brearley and de Mestre (1996) and Brearley et al. (1998). In order to develop the five segment kinematic model used in this investigation, the kinematic relationships of the ankles, knees, hips, shoulders, elbows and hands must be modeled based on measured data, in order to determine the velocities of the centre of mass locations of each body segment.

3.1. Determination of limb centre of mass locations

Winter (1990) presented standard anthropometric data that allows for the determination of limb lengths, limb masses, and limb centre of mass locations, based on the mass and height of the subject. Through knowledge of the joint trajectories occurring during each stroke and the mean height and combined mass of the crew, using this anthropometric data, the centre of mass coordinates could be calculated. As only the horizontal joint trajectories will influence horizontal boat propulsion, only the longitudinal components (x-components) of these trajectories are required, and these are derived below.

It is assumed that the stretcher position is the same for all crew members. Therefore, the ankle is assumed to be at the coordinates (0,0) for all crew members, as it is fixed in relation to the boat. The

coordinates of the knee, K_x, and elbow, E_x, can be determined through knowledge of the x-coordinates of the ankle, A_x, and hip, H_x, and of the shoulder, S_x, and hand, Hd_x, respectively and by taking the ratio of 'shank length : leg length' and 'forearm length : arm length', respectively, such that the coordinates are given by,

$$K_x = \frac{0.246}{0.491}\left(H_x - A_x\right) \tag{3}$$

$$E_x = \frac{0.146}{0.332}\left(S_x - Hd_x\right) \tag{4}$$

The trajectories of the hip, shoulder and hand are based on measured data and will be discussed below. The x-positions of the centre of mass of the lower leg, C_{shank}, thigh, C_{thigh}, trunk, C_{trunk}, upper arm, C_{arm}, and forearm, $C_{forearm}$, were defined by,

$$C_{shank} = 0.567\left(K_x - A_x\right) + A_x \tag{5}$$

$$C_{thigh} = 0.567\left(H_x - K_x\right) + K_x \tag{6}$$

$$C_{trunk} = 0.5\left(S_x - H_x\right) + H_x \tag{7}$$

$$C_{arm} = 0.436\left(E_x - S_x\right) + S_x \tag{8}$$

$$C_{forearm} = 0.682\left(H_x - E_x\right) + E_x \tag{9}$$

respectively.

3.2. Modeling limb movement forces

Equation (2) shows that the force, F_{crew}, exerted on the boat due to the movement of the crew relative to the boat is given by,

$$F_{crew} = M\frac{dv_{crew}}{dt} \tag{10}$$

In order to account for the different velocities of individual body segments, this must now be written such that,

$$F_{crew} = 2\left(F_{shank}\right) + 2\left(F_{thigh}\right) + F_{trunk} + 2\left(F_{arm}\right) + 2\left(F_{forearm}\right) \tag{11}$$

where the force exerted by the lower leg (shank), F_{shank}, thigh, F_{thigh}, trunk, F_{trunk}, upper arm, F_{arm}, and the forearm, $F_{forearm}$, are given by,

$$F_{shank} = 0.0465M\frac{d^2C_{shank}}{dt^2} \tag{12}$$

$$F_{thigh} = 0.1M\frac{d^2C_{thigh}}{dt^2} \tag{13}$$

$$F_{trunk} = 0.578M\frac{d^2C_{trunk}}{dt^2} \tag{14}$$

$$F_{arm} = 0.028M\frac{d^2C_{arm}}{dt^2} \tag{15}$$

$$F_{forearm} = 0.022M\frac{d^2C_{forearm}}{dt^2} \tag{16}$$

respectively. Substituting equation (14) into equation (2), the equation of motion for the boat can now be written as

$$\frac{dv_{shell}}{dt} = \left(P - D - F_{crew}\right)/\left(m + M\right) \tag{17}$$

4. Experimental data collection

In order to model the crew joint trajectories to drive the five segment model of crew movement, the movement patterns seen in rowing must be determined experimentally. The following section details the experimental aspect of this paper, and shows how a kinematic relationship was developed to model

mathematically the measured motion of the rowers.

4.1. Methods

Nine male senior club rowers took part in the study. The rowers had a mean age, height and body mass of 21.9 (±1.2) years, 1.81 (±0.07) m, and 83.4 (±7.8) kg, respectively. Subjects had 5.6 (±2.8) years experience in competitive on-water rowing and were a combination of lightweight and heavyweight rowers and scullers. The study was approved by the local ethics sub-committee of the University of Birmingham, and subjects gave written informed consent prior to their participation.

A motion capture system (Vicon, Oxford Metrics Ltd., UK) was used to measure the motion of the rowers' body segments throughout each stroke whilst rowing on a rowing ergometer (Concept 2 model C, Concept 2, Morrisville). 35 reflective markers (diameter = 0.025 m) were attached to each subject. The marker positions were selected in order to allow for the calculation of the joint coordinates at the ankles, hips shoulders and hands. Six infrared cameras (Vicon 8, Oxford Metrics Ltd., UK) detected the position of each marker and the data was sampled at 120 Hz by the Vicon "datastation" (Vicon 512, Oxford Metrics Ltd., UK) before being stored on a workstation computer for later analysis.

The rowing ergometer was instrumented to measure handle velocity using a DC tachometer (263-6005, RS Components, UK). The tachometer enabled measurement of the rotational velocity of the ergometer chain sprocket (pitch diameter = 2.83 cm), from which linear handle velocity could be calculated to a resolution of 0.07%. The analogue signal was sampled at 120 Hz and passed to the Vicon Workstation via an analogue-to-digital board (Vicon, Oxford Metrics Ltd., UK).

During each stroke, the oar handle position oscillates back and forth. This causes the handle velocity to change from being positive during the drive phase to being negative during the recovery phase. The catch and finish of each stroke were therefore defined as when the oar handle velocity changed sign.

Subjects performed their normal warm up for a period of approximately 4 minutes on the rowing ergometer. This period was used to ensure that the subjects were comfortable with the markers attached to them, and that the markers were attached securely. The drag factor on the ergometer was set by each rower in order to match the drag they were used to during normal training. Subjects were then asked to row at 30 strokes per minute for 30 seconds. Data collection commenced once each subject had reached a stroke rate of 30 strokes per minute and each subject was encouraged to maintain their normal rowing technique throughout.

Due to the linear nature of rowing movements on the Concept 2 rowing ergometer only the joint trajectories in the horizontal (x) direction were required, and joint trajectories for the left and right side of the body were averaged to give a mean trajectory for each joint. Joint trajectories for fifteen strokes for each subject were analyzed, and subsequently split into drive and recovery phases before being normalized in the time domain. All normalized drive and recovery phases were averaged for each variable across all subjects.

4.2. Results and discussion

Fig. 2 shows that the hip continued moving until approximately 75% through the drive phase (as indicated by the arrow). This lack of hip movement towards the end of the drive shows that the legs are fully extended before the end of the phase, which would result in the force applied to the boat decreasing at this stage, due to the legs providing most of the source of power (Kleshnev & Kleshneva, 1992), thus reducing boat acceleration. The shoulder continued to move until approximately 85% through the drive, and the hand continued to move for the entire duration of the drive phase. The timings of joint movements observed here illustrate the importance of modeling the movement of each body segment individually in determining the momentum exchanges occurring between the crew and boat. As the ankles remained fixed in the boat and the knee and elbow trajectories are dependent on the locations of the hip, shoulder and hand, respectively, they are not shown here.

4.3. Modeling measured joint trajectories

In order to calculate the centre of mass trajectories of each segment in the x-direction, the measured trajectories of the hips, shoulders and hands shown in Fig. 2 were modeled as cosine functions of time, which were scaled according to the catch and finish joint coordinates in the x-axis, and also according to the duration of body segment movement during the drive and recovery phases. The relationships are given by,

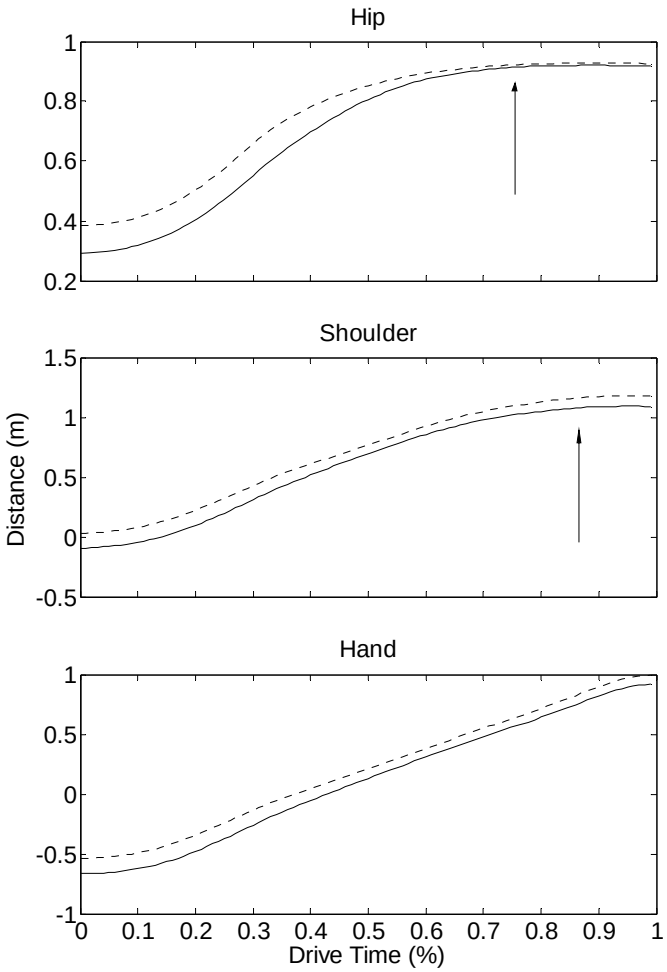

Fig. 2. Measured x-trajectories of the hip, shoulder and hand during the drive phase of the stroke for ergometer rowing, showing the mean (—) and standard deviation (---) for the nine sub-elite rowers used.

$$H_x = \left[0.5\left(-\cos\left(\frac{4\pi t}{3\tau_1}\right)\right)+1\right]\times\left(H_{x_{finish}} - H_{x_{catch}}\right)+ H_{x_{catch}} \tag{18}$$

$$S_x = \left[0.5\left(-\cos\left(\frac{6\pi t}{5\tau_1}\right)\right)+1\right]\times\left(S_{x_{finish}} - S_{x_{catch}}\right)+ S_{x_{catch}} \tag{19}$$

$$Hd_x = \left[0.5\left(-\cos\left(\frac{\pi t}{\tau_1}\right)\right)+1\right]\times\left(Hd_{x_{finish}} - Hd_{x_{catch}}\right)+ Hd_{x_{catch}} \tag{20}$$

respectively, where the maximum and minimum x-coordinates of each joint being denoted by the subscripts catch and finish, respectively, t is the total stroke time and τ_1 is the drive duration. Using the measured catch and finish positions, the trajectories of the hips, shoulders and hands were calculated by substituting these positions into equations (3) to (5) (see Fig. 3). Trajectories for the recovery phase could be modeled adequately by the same relationships as for the drive and so are not shown.

For the validity of the simulation, it was important to ensure that the observed errors between measured and modeled trajectories (Fig. 3) were less than the differences measured between rowers (Fig. 2). Table 1 illustrates that the error between measured and modeled trajectories falls within the limits of the differences found in the measured data. From the modeled hip, shoulder and hand trajectories, the limb centre of mass coordinates and the forces imparted on the boat through limb movement could then be determined as discussed earlier.

Table 1. Maximum standard deviations for measured trajectories and between measured and modelled trajectories.

	Measured trajectories standard deviation (m)	**Measured vs. modeled trajectories standard deviation (m)**
Hip	0.11	0.04
Shoulder	0.13	0.04
Hand	0.14	0.10

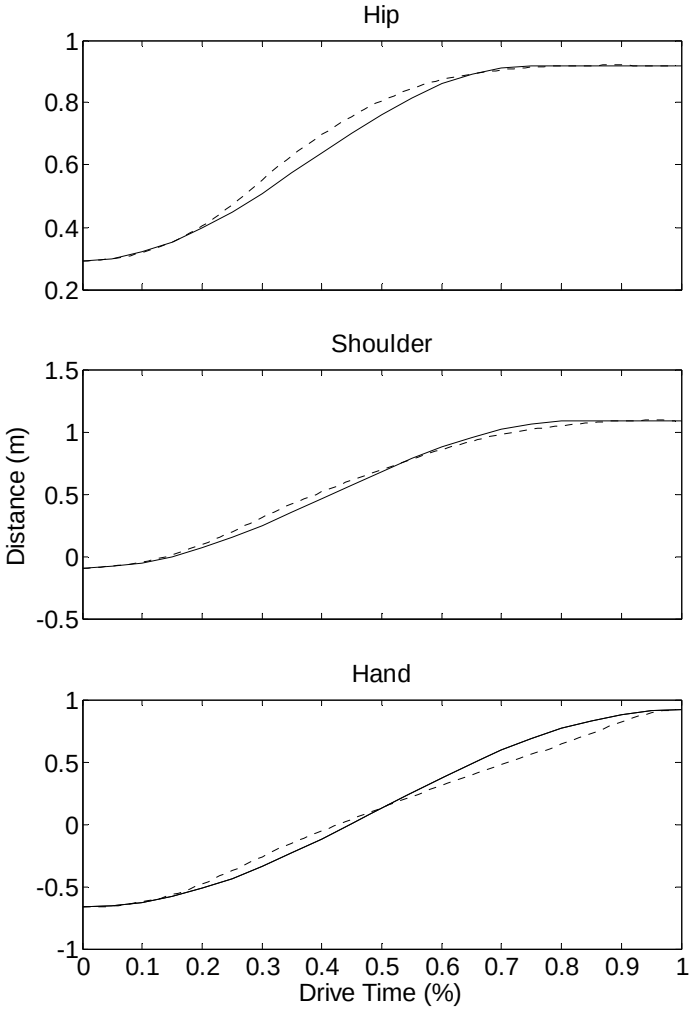

Fig. 3. Modelled trajectories (—), calculated by equations (3) – (5), of the hip, shoulder and hand are shown for the drive phase of the rowing stroke. Measured trajectories (---) presented in Fig. 2 are also shown.

5. Simulations

The model was built in Simulink (Matlab, Mathworks, USA), and solved using the inbuilt Runge-Kutta variable-rate solver with a maximum time step of 0.005 seconds. This was chosen as it was found to provide the highest level of accuracy of all the available solvers. Each section of the model was checked manually to ensure it produced true results. The model provided a continuous output of all variables with time.

5.1. Validation against mean steady state on-water boat velocities

For validation of the present model, model outputs were compared to measured on-water data that was provided for a heavyweight men's eight (Kleshnev, 1999), as done previously (Caplan & Gardner, 2007b). Data for four stroke rates were available, and input variables for the model were matched to those of the measured data (Table 2). The lift and drag coefficients required to solve the model were taken from Caplan

and Gardner (2007a) for a Big Blade. It was assumed that there was no wind or water current, and the oars were assumed to be without mass (Brearley & de Mestre, 1996; Brearley et al., 1998; Caplan & Gardner, 2007b).

Table 2. Input variables for validation against measured data for an eight.

Variable	**28.8 spm**	**30.6 spm**	**32.1 spm**	**35.3 spm**
Total time (s)	2.08	1.96	1.87	1.70
Drive time (s)	0.94	0.92	0.88	0.83
Recovery time (s)	1.14	1.04	0.99	0.87
Number of rowers	8	8	8	8
Rower mass (kg)	92.5	92.5	92.5	92.5
Shell + coxswain mass (kg)	146	146	146	146
Slide amplitude (m)	0.36	0.36	0.36	0.36
Outboard oar length (m)	2.365	2.365	2.365	2.365
Oar blade design	Big Blade	Big Blade	Big Blade	Big Blade
Blade area (m^2)	0.124	0.124	0.124	0.124

To avoid error in determining the rotational inertia of the oar to determine its angular motion using pull force and blade force (i.e. $\sum$Moments = $I\alpha$), the simpler option of driving the model through blade motion was adopted (Caplan & Gardner, 2007b). This avoided inaccuracy in the approximation of rotational inertia arising from variation in the shaft cross sectional shape and area along its length. The selected procedure entailed using the normalized measured oar shaft relationships (Kleshnev, 1999) as model input, which were matching between stroke rates. This allowed the motion of the oar blade to be determined throughout the stroke and therefore the oar blade force imparted on the water to propel the boat. The modeled rower kinematic relationships discussed above were used in the five segment model and a rower movement amplitude of 0.36m was used for the single segment model, as used previously (Brearley & de Mestre, 1996; Brearley et al., 1998; Caplan & Gardner, 2007b).

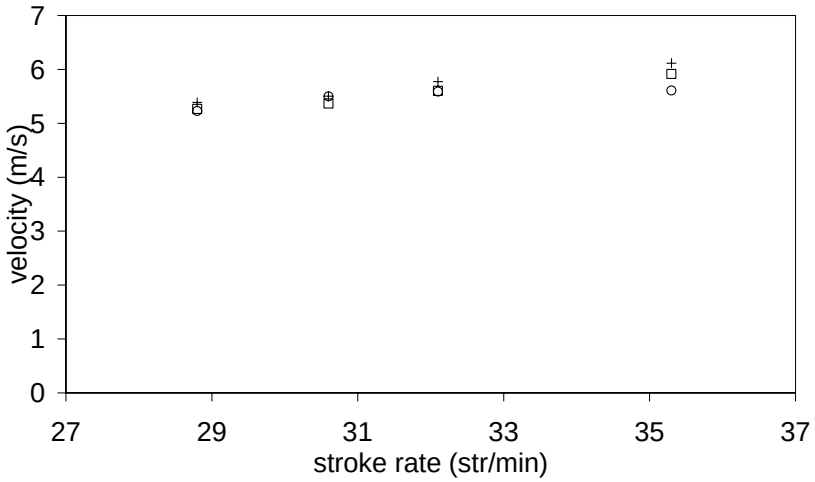

Figure 4. Validation of 5 segment model (□) and single segment model (+) against the measured (○) on-water rowing mean boat velocity at four stroke rates (Kleshnev, 1999).

Figure 4 shows the validation of both the five segment and single segment models against measured on-

water mean steady state boat velocity (Kleshnev, 1999). A very close approximation was seen between both the modeled mean velocities and the measured data between 29 and 32 strokes per minute. At 35.3 strokes per minute the difference was a little more pronounced for both models, although it was less than 10% of the measured mean boat velocity. This can be attributed to minor environmental influences such as water current or wind, which were not measured by Kleshnev (1999) and therefore were not simulated by the model. The five segment model achieved a closer approximation of measured data than the single segment model, with the single segment model predicting velocities approximately 3% greater than the five segment model.

5.2. Influence of model type on instantaneous boat velocity

The input variables shown in Table 3 were used as input to both the single and five segment models. The stroke rate used corresponded to the stroke rate maintained in the kinematic data collection discussed above.

Table 3. General input variables for all simulations.

Variable	Value
Stroke rate (strokes/minute)	30
Total time (s)	2
Drive time (s)	0.92
Recovery time (s)	1.08
Drive/total time ratio (%)	46
Number of rowers	8
Rower height (m)	1.92
Rower mass (kg)	92.5
Combined rower mass (kg)	740
Combined boat + coxswain mass (kg)	146
Outboard oar length (m)	2.365
Oar blade	Big Blade
Water temperature (ºC)	16
Blade area (m^2)	0.124

Figure 5 shows the instantaneous boat velocity for both models. Boat velocity started slower at the catch for the single segment model, but was seen to decrease more rapidly with the five segment model and reach a slower minimum velocity. In the five segment model, the legs move through their full range during only the first 75% of the drive and the trunk during only the first 85% (Fig. 2). This will result in the velocity peaks occurring earlier in the drive compared to the single segment model where the velocity peak will be reached mid-way through the drive. These differences can also be seen to influence the velocity towards the end of the drive phase where the lack of leg extension and trunk movement in the five segment model in the last 15-20% of the drive cause a reduction in the acceleration of the boat, a feature not present for the single segment model boat velocity, but present in the measured data from Kleshnev (1999) in Figure 1.

During the recovery phase, there is a delay to the start of knee flexion in the five segment model until the hands pass the knees. This can be seen to influence the rate of increase in boat velocity at the start of the recovery in the five segment model, but due to the single segment model assuming an even distribution of rower movement throughout the recovery, an immediate increase in boat velocity is seen, which does not correspond to the features of measured on-water boat velocities (Fig. 1).

5.3. Model limitations

Although the model achieved a good agreement with measured on-water rowing data, there are a number of limitations which must be acknowledged. First, the human body is far more complex than the five segment kinematic model used here. Each segment of the upper and lower limbs are not rigid segments and the spine flexes during the stroke. However, for the purposes of examining the influence of crew technique on boat velocity fluctuations, these factors will have only a very small impact. Future work should look more closely at modeling spinal flexion and extension through the stroke. Second, the motion of the foot is ignored. Only the front of the foot is attached to the stretchers, and the heel is free to raise away from the stretchers. For a more complete model of crew movement, this should also be considered.

The use of ergometer kinematic relationships to predict on-water rowing performance is not ideal. However, rowing ergometers have been shown to closely approximate on-water rowing. In fact, Lamb (1989) showed there to be no significant kinematic differences between the two rowing forms, except for the movement of the arms at the catch and finish, and Dawson et al. (1998) showed that drive phase to recovery phase duration ratio varied with stroke rate in the same way for both on-water and ergometer rowing.

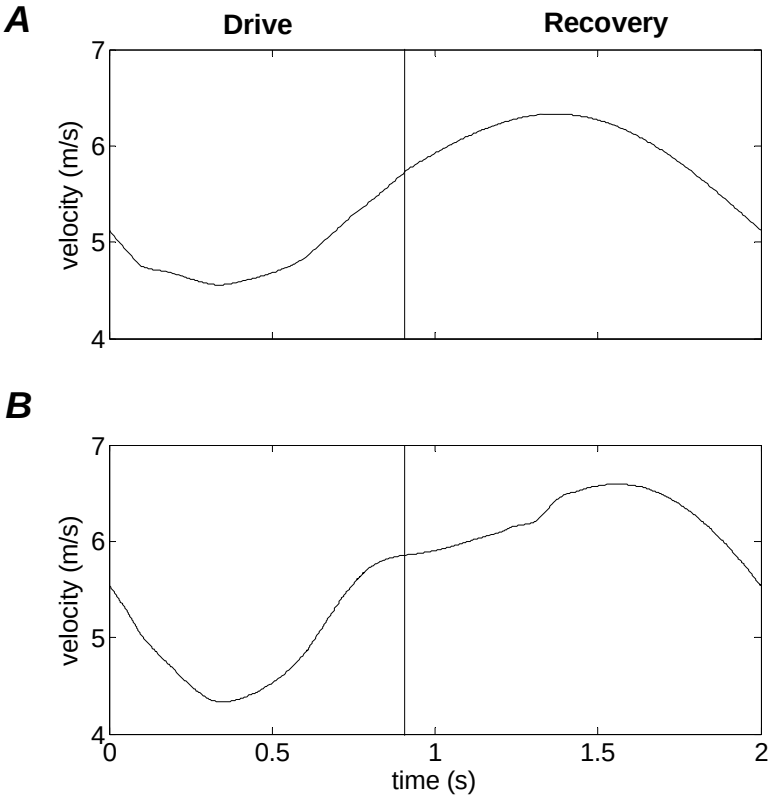

Fig 5. Instantaneous boat velocity is shown for one complete stroke for the single segment model (A) and the five segment model (B). Drive and recovery phases are indicated with the catch indicated by the left (t=0) and right (t=2) axes. The finish is indicated by the vertical line at t=0.92. An exact comparison with measured on-water data was not appropriate due to the different rower kinematic relationships used which were not available for the measured on-water data.

6. Conclusions

The present investigation aimed to investigate the validity of using a single segment model of crew movement during the rowing stroke on both mean and instantaneous boat velocity. Kinematic relationships were measured for rowers which allowed for the development of a five segment kinematic model of crew movement. Both the single segment and five segment models were shown to be valid against measured mean steady-state on-water boat velocity, although the single segment model was observed to predict a higher mean velocity (approximately 3%) than the five segment model and the measured data. The five segment model, however, was the only model to predict the key features of instantaneous boat velocity seen during real on-water rowing, such as the reduction in boat acceleration towards the end of the drive phase

and the delayed increase in boat velocity at the start of the recovery.

Despite the limitations of the current model discussed in the previous section, this development of the model could have practical application for rowers, coaches and sports scientists, as it has been shown to be valid in using individual rower kinematics to estimate the influence of their technique (or technique changes) on both mean boat velocity and the velocity profile during each stroke. The influence on boat velocity fluctuations of technique errors such as "rushing the slides", which can cause a "checking" of boat velocity at the end of the recovery, could therefore be examined using the model in order to provide feedback to rowers for improving technique.

7. References

[1] K. Affeld, K. Schichl, & A. Ziemann, Assessment of rowing efficiency. *International Journal of Sports Medicine.* 1993, **14**(1): S39-S41.

[2] R. S. Barrett, & J. M. Manning. Relationships between rigging set-up, anthropometry, physical capacity, rowing kinematics and rowing performance. *Sports Biomechanics*. 2004, **3**: 221-235.

[3] M. N. Brearley, & N. J. de Mestre, Modelling the rowing stroke and increasing its efficiency. 3rd conference on mathematics and computers in sport, Bond University, Queensland, Australia, 1996, 35-46.

[4] M. N. Brearley, N. J.de Mestre, & D. R. Watson. Modelling the rowing stroke in racing shells. *The Mathematical Gazette*. 1998, **82**: 389-495.

[5] D. Cabrera, A. Ruina, & V. Kleshnev. A simple 1+ dimensional model of rowing mimics observed forces and motions. *Human Movement Science*. 2006, **25**: 192-220.

[6] N. Caplan, & T. N. Gardner. The influence of stretcher height on the mechanical effectiveness of rowing. *Journal of applied biomechanics*. 2005, **21**: 286-296.

[7] N. Caplan, & T. N.Gardner, A fluid dynamic investigation of the Big Blade and Macon oar blade designs in rowing propulsion. *Journal of Sports Sciences*. 2007, **25**: 643-650.

[8] N. Caplan, & T. N. Gardner, A mathematical model of the oar blade-water interaction in rowing. *Journal of Sports Sciences*. 2007, **25**: 1025-1034.

[9] N. Caplan, & T. N. Gardner. Optimization of oar blade design for improved performance in rowing. *Journal of Sports Sciences*. 2007.

[10] F. Colloud, S. Manel, & A. H. Rouard. 3D kinematic relationships between blade and boat in rowing. *Journal of Human Movement Studies.* 2001, **40**: 83-100.

[11] R. G. Dawson , R. J. Lockwood, J. D. Wilson, & G. Freeman, The rowing cycle: Sources of variance and invariance in ergometer and on-the-water performance. *Journal of Motor Behaviour*, 1998, **30**: 33-43.

[12] E. H. Elliott , J. Hamill, , & T. R. Derrick, In-shoe pressure distribution during ergometer rowing in novice and experienced rowers. Proceedings of the XI International Symposium on Biomechanics in Sport. Amherst, Massachusetts. 1993, 349-352.

[13] U. Hartmann, A.Mader, K. Wasser, , & I. Klauer, Peak force, velocity, and power during five and ten maximal rowing ergometer strokes by world class female and male rowers. *International Journal of Sports Medicine,* 1993, **14**(1): S42-S45.

[14] D. Hawkins, A new instrumentation system for training rowers. *Journal of Biomechanics*, 2000, **33**: 241-245.

[15] S. F. Hoerner, Fluid-dynamic drag. Albuquerque, New Mexico: *Hoerner Fluid Dynamics*, 1965.

[16] P. J. E. Holt, A. M. J. Bull, P. M. M. Cashman, & A. H. McGregor. Kinematics of spinal motion during prolonged rowing. *International Journal of Sports Medicine*. 2003, **24**: 597-602.

[17] V. Kleshnev. Propulsive efficiency of rowing. R.H.Sanders & N. R. Gibson (Eds.), XVII International Symposium on Biomechanics in Sports. Perth: School of Biomedical and Sport Science, Edith Cowan University, 1999, 224-228.

[18] V. Kleshnev, & E. Kleshneva. *Work performance of different body segments of rowers. Biology of Sport*. 1992, **9**: 127-133.

[19] D. H. Lamb. A kinematic comparison of ergometer and on-water rowing. *American Journal of Sports Medicine*. 1989, **17**: 367-373.

[20] T. P. Martin, & J. S. Bernfield. Effect of stroke rate on velocity of a rowing shell. *Medicine and Science in Sports and Exercise.* 1980, **12**: 250-256.

[21] A. H. McGregor, A. M. J. Bull, & R. Byng-Maddick. A comparison of rowing technique at different stroke rates: a description of sequencing, force production and kinematics. *International Journal of Sports Medicine*. 2004, **25**: 465-470.

[22] A. Millward. A study of the forces exerted by an oarsman and the effect on boat speed. *Journal of Sports Sciences*. 1987, **5**: 93-103.

[23] V. Nolte. Do you need hatchets to chop your water? *American Rowing*, July/August. 1993, 23-26.

[24] F.O'Brien. The design of racing rowing boats. *Computer Aided Design*. 1970, 3-8.

[25] K.Owen, G. Whyte, S. A. Ingham , & C. Waygood. Maximal force and power output of elite heavyweight and lightweight male rowers. *Journal of Sports Sciences*, 2002, **20**: 14.

[26] T. W. Pelham, L. E. Holt, K. Burton, A. G. W. Carter, & J. P. Peach. The effect of oar design on scull boat dynamics. *Proceedings of the XI international symposium on biomechanics in sports. Amherst, Massachusetts*. 1993, 201-204.

[27] C. A. Scragg, & B. D. Nelson. The design of an 8 oared rowing shell. *Marine Technology and Sname News*, 1993, **30**: 84-99.

[28] R. M. Smith & C. Loschner. Biomechanics feedback for rowing. *Journal of Sports Sciences*. 2002, **20**: 783-791.

[29] R. M. Smith & W. L. Spinks, Discriminant analysis of biomechanical differences between novice, good and elite rowers. *Journal of Sports Sciences*. 1995, **13**: 377-385.

[30] R. M. Smith & W. L. Spinks. A system for the biomechanical assessment of rowing performance (ROWSYS). *Journal of Human Movement Studies*. 1998, **34**: 141-157.

[31] W. L. Spinks. Force-angle profile analysis in rowing. *Journal of Human Movement Studies*. 1996, **31**: 211-233.

[32] J. F. Wellicome. Report on resistance experiments carried out on three racing shells. *National Physical Laboratory Ship Division Technical Memorandum*. 1967, 184.

[33] D. A. Winter, Biomechanics and motor control of human mo*vement*. Canada: John Wiley & Sons, Inc, 1990.